

# Exosomes derived from baicalin-pretreated mesenchymal stem cells mitigate atherosclerosis by regulating the SIRT1/NF- $\kappa$ B signaling pathway

XIAOCHUN YANG<sup>1\*</sup>, WEI WU<sup>1\*</sup>, WEITIAN HUANG<sup>2</sup>, JUNFENG FANG<sup>3</sup>,  
YUNLI CHEN<sup>2</sup>, XIAOYAN CHEN<sup>2</sup>, XIAOLAN LIN<sup>2</sup> and YANBIN HE<sup>2</sup>

<sup>1</sup>The First Clinical College of Medicine, Guangzhou University of Chinese Medicine, Guangzhou, Guangdong 510405, P.R. China;

<sup>2</sup>Department of Rehabilitation, Guangdong Work Injury Rehabilitation Hospital, Guangzhou, Guangdong 510000, P.R. China;

<sup>3</sup>Department of Emergency, The First Affiliated Hospital of Guangzhou University of Chinese Medicine, Guangzhou, Guangdong 510000, P.R. China

Received October 15, 2024; Accepted February 13, 2025

DOI: 10.3892/mmr.2025.13491

**Abstract.** Atherosclerosis (AS) is a disease with high global incidence and mortality rates. Currently, the treatment of AS in clinical practice carries a high risk of adverse effects and toxic side effects. The pretreatment of mesenchymal stem cells (MSCs) with drugs may enhance the bioactivity of MSC-derived exosomes (MSC-exos), which could be a promising candidate for inhibiting the progression of AS. The aim of the present study was to investigate the ability of exos derived from baicalin-preconditioned MSCs (Ba-exos) to exhibit an inhibitory effect on AS progression and to explore the potential molecular mechanisms. Exos were isolated from untreated MSCs and MSCs pretreated with Ba, and were characterized using transmission electron microscopy, nanoparticle tracking analysis and western blotting. Subsequently, Cell Counting Kit-8 and Transwell assays, reverse transcription-quantitative PCR, immunofluorescence, western blotting and ELISA were used to evaluate the effects of Ba-exos on AS, and the possible molecular mechanisms. Oil Red O and Masson staining were used to assess AS pathological tissue in a high-fat diet-induced mouse model of AS. Notably, MSC-exos and Ba-exos were successfully isolated. Compared with MSC-exos, Ba-exos demonstrated superior inhibitory effects on the viability and migration, and the levels of inflammatory factors in oxidized low-density lipoprotein (ox-LDL)-induced vascular smooth muscle cells (VSMCs).

Additionally, compared with MSC-exos, Ba-exos significantly inhibited NF- $\kappa$ B activation by upregulating sirtuin 1 (SIRT1), thereby suppressing inflammation in ox-LDL-induced VSMCs to a greater extent. In mice with high-fat diet-induced AS, Ba-exos exhibited the ability to inhibit AS plaque formation and to alleviate AS progression by reducing the levels of inflammatory factors compared with MSC-exos; however, the difference was not significant. In conclusion, Ba-exos may serve as a potential strategy for treating AS by regulating the SIRT1/NF- $\kappa$ B signaling pathway to suppress inflammation.

## Introduction

Atherosclerosis (AS) is a type of chronic metabolic disease characterized by the deposition of lipid plaques on the inner wall of large and medium-sized arteries, leading to arterial hardening and other secondary pathological changes, which has high incidence and mortality rates worldwide (1). The pathogenesis of AS is complex and involves various pathological processes, including abnormal endothelial cell function, lipid deposition, vascular smooth muscle cell (VSMC) proliferation and migration, and inflammatory reactions (1,2). At present, the clinical treatment of AS mainly includes lifestyle interventions (3), lipid-lowering therapy (4) and anti-thrombotic treatment (5). Notably, these therapies mainly rely on frequent systemic injections, which lead to unexpected side effects. For example, lipid-lowering statins can cause muscle pain and liver toxicity in some patients, whereas anti-thrombotic drugs such as aspirin may lead to gastrointestinal bleeding (6,7). Therefore, there is a need to develop new drugs with high delivery specificity and fewer off-target effects.

NF- $\kappa$ B is a dimer composed of two protein subunits, p50 and p65, which is expressed in almost all animal cells and serves as a convergence point for multiple signaling pathways, playing a crucial role in the occurrence and development of inflammation (8). NF- $\kappa$ B can induce the excessive or sustained expression of cytokines, such as TNF- $\alpha$  and IL-6, adhesion factors and chemotactic factors, promoting inflammatory reactions in diseases (9,10). It has previously been shown that the

*Correspondence to:* Dr Yanbin He, Department of Rehabilitation, Guangdong Work Injury Rehabilitation Hospital, 68 Kai Tak Road, Guangzhou, Guangdong 510000, P.R. China  
E-mail: heyb\_17@sina.com

\*Contributed equally

**Key words:** exosomes, mesenchymal stem cells, baicalin, atherosclerosis, inflammation

upregulation of NF- $\kappa$ B is closely related to the occurrence of cardiovascular diseases (11). In addition, inflammation induced by oxidized low-density lipoprotein (ox-LDL) is an important event in the progression of AS (12). Multiple studies have shown that ox-LDL can promote NF- $\kappa$ B activation, further accelerating the occurrence and development of AS (13,14). Sirtuin 1 (SIRT1) is a member of the NAD-dependent deacetylase family, which can affect inflammatory reactions by regulating the deacetylation of transcription factors, proteins and histones (15). Research has shown that SIRT1 inhibits inflammatory reactions through interaction with the RelA/p65 subunit of NF- $\kappa$ B (16). A recent study has shown that dihydromyricetin suppresses the polarization of proinflammatory cells-M1 macrophages and alleviates the progression of AS by regulating the SIRT1/NF- $\kappa$ B signaling pathway (17). These previous findings suggest that activating SIRT1, blocking NF- $\kappa$ B signaling and inhibiting inflammatory reactions during the progression of AS may be a key strategy for its treatment.

Mesenchymal stem cell (MSC)-based therapies have been shown to exert strong anti-inflammatory and immune-regulatory effects in various pathological processes of cardiovascular diseases (18). Notably, the paracrine function of MSCs serves an important role in cardiovascular disease progression. Exosomes (exos) are membrane-derived nanosized vesicles (size range, 30-200 nm), which serve as the main form of paracrine secretion of MSCs. They contain bioactive substances, such as nucleic acids, proteins and lipids, mediating intercellular communication and serving important roles in physiological and pathological processes (19). Increasing evidence has revealed that MSC-derived exos (MSC-exos) have beneficial effects in AS. Zhang *et al* (20) showed that MSC-exos can reduce plaque formation in ApoE-knockout mice with AS through FENDRR. Ma *et al* (21) demonstrated that MSC-exos can promote M2 macrophage polarization and reduce macrophage infiltration to alleviate AS by delivering microRNA (miRNA/miR)-21a-5p to macrophages. However, the mechanism by which MSC-exos exert protective effects through regulation of the SIRT1/NF- $\kappa$ B signaling pathway and the inhibition of inflammation in AS remains unclear.

It has been reported that pretreatment with cytokines, drugs, hypoxia or physical factors can improve the transplantation efficacy of MSC-exos, enhance the biological functions of MSCs and prepare them with the desired characteristics (22). For example, hypoxic preconditioning can increase the secretion of anti-inflammatory cytokines from MSCs (23), whereas apelin pretreatment can enhance the cardioprotective effects of MSCs (24). Baicalin (Ba) is one of the most abundant active ingredients extracted from the dried roots of *Scutellaria baicalensis*, a Chinese herbal medicine; it has various pharmacological effects, including anti-inflammatory, antimicrobial, antifibrotic, antioxidant and anticancer activities (25-27). Notably, several studies have revealed the potential of Ba in the prevention and treatment of AS. Ba has been shown to target high mobility group box 1 and to upregulate miR-126-5p, which can inhibit the proliferation and migration of ox-LDL-VSMCs, thus alleviating AS (28). Furthermore, Ba alleviates oxidative stress and inflammation by deactivating the NF- $\kappa$ B and p38 MAPK signaling pathways, thus relieving AS (29). However, the benefits of exos derived from Ba-preconditioned MSCs (Ba-exos) in AS are still unclear.

The current study aimed to investigate the potential role of Ba-exos in alleviating the progression of AS using both *in vivo* and *in vitro* models. Furthermore, the key mechanisms by which Ba-exos alleviate AS progression through regulation of the SIRT1/NF- $\kappa$ B signaling pathway and the inhibition of inflammation were investigated further. The current study elucidated the potential advantages of Ba-exos in the progression of AS, and provides an effective and promising approach to optimize the treatment process of MSC-exos in AS.

## Materials and methods

**Cell culture.** Mouse aortic VSMCs (cat. no. CP-M076) and mouse adipose-derived MSCs (cat. no. CP-M138) were purchased from Wuhan Pricella Biotechnology Co., Ltd. The use of primary cells was approved by the Experimental Animal Ethics Review Committee of the Guangdong Work Injury Rehabilitation Hospital (approval no. GDWIRH2023044; Guangzhou, China). The cells were cultured in RMPI-1640 medium (Thermo Fisher Scientific, Inc.) supplemented with 10% fetal bovine serum (Thermo Fisher Scientific, Inc.), 100 U/ml penicillin and 0.1 mg/ml streptomycin. The cells were maintained in a CO<sub>2</sub> incubator at 37°C with 5% CO<sub>2</sub>. The culture medium was replaced every day and subculturing was performed when cells reached ~85% confluence. In addition, the medium of MSCs was supplemented with 1  $\mu$  M Ba (MedChemExpress) and incubated at 37°C for 48 h for the subsequent isolation of exos.

**Collection and purification of MSC-exos.** When MSCs reached 80% confluence, they were cultured in serum-free medium for 24 h to collect the cell supernatant. The exos were collected using differential centrifugation. Firstly, the collected cell supernatant was centrifuged at 300 x g for 10 min at 4°C, followed by centrifugation at 2,000 x g for 10 min at 4°C, and then at 10,000 x g for 30 min at 4°C to obtain the supernatant. The supernatant was filtered through a 0.22- $\mu$ m filter and transferred to an ultracentrifuge tube. The precipitate was collected by centrifugation at 12,000 x g for 70 min at 4°C and resuspended in PBS. The resuspended precipitate was then centrifuged again at 12,000 x g for 70 min at 4°C, and the obtained precipitate was resuspended in an appropriate amount of PBS and stored at -80°C for further study.

**Identification and characterization of exos.** A total of 10  $\mu$ l exo sample was added to an equal volume of 2.5% glutaraldehyde and incubated at room temperature for fixation on a transmission electron microscope (TEM) grid for 2 min. The samples were then embedded in epoxy resin at 60°C for 24 h and sectioned into 70-nm ultrathin slices. Subsequently, 3% phosphotungstic acid was added and the grid was stained at room temperature for 2 min. The grid was then washed with distilled water and images were captured under a TEM (TM4000plusII; Hitachi, Ltd.). In addition, 5  $\mu$ l exo sample was diluted with PBS to a 1,000-fold dilution for particle size analysis using a nanoparticle tracking analyzer (NTA; NanoSight Pro; Malvern Panalytical, Ltd.). The expression levels of the specific marker proteins TSG101 (1:2,000; cat. no. 28283-1-AP), CD9 (1:1,000; cat. no. 20597-1-AP) and CD63 (1:1,000; cat. no. 32151-1-AP) all from Proteintech Group, Inc.) in exos were detected by

western blotting; the membranes were incubated with these primary antibodies at 4°C overnight.

**VSMC grouping and intervention methods.** Third-generation VSMCs with good growth status were cultured in a 6-well plate ( $1 \times 10^5$  cells/well) containing DMEM (Thermo Fisher Scientific, Inc.) supplemented with 100 mg/l ox-LDL (cat. no. 20605ES05; Shanghai Yeasen Biotechnology Co., Ltd.) and incubated for 24 h; this was designated as the ox-LDL group. Cells cultured in DMEM without ox-LDL served as the control group. After 24 h of ox-LDL induction, 50  $\mu$ g MSC-exos or 50  $\mu$ g Ba-exos were added to the ox-LDL + MSC-exos group and the ox-LDL + Ba-exos group, respectively (30). In addition, small interfering RNA (si)-negative control (NC)- or si-SIRT1-transfected Ba-exos were co-cultured with VSMCs for 48 h, which were designated as the Ba-exos + si-NC group and the Ba-exos + si-SIRT1 group, respectively. For transfection, a total of  $1 \times 10^6$  cells were seeded into a cell culture plate and transfected with 50 nM siRNA using Lipofectamine<sup>®</sup> 2000 reagent (Invitrogen; Thermo Fisher Scientific, Inc.) at room temperature for 48 h, strictly following the manufacturer's protocol. The transfection efficiency was evaluated by reverse transcription-quantitative PCR (RT-qPCR) analysis 48 h post-transfection. The siRNA sequences that were used were as follows: si-NC sense, 5'-CAGGAGGUUACGCGCAAGUUC-3' and antisense, 5'-ACUUGAGCGUCCAAACCUGAU-3'; si-SIRT1 sense, 5'-UGAACAAAAGUAUAUGGACCU-3' and antisense, 55'-GUCCAUAUACUUUUGUUCAGC-3'.

**Cell counting kit-8 (CCK-8) assay.** VSMCs in logarithmic growth phase were digested with 0.25% trypsin, centrifuged at  $100 \times g$  for 5 min at 4°C, resuspended and counted. The cells were then adjusted to a concentration of  $10^3$  cells/l and were seeded into a 96-well plate at 200  $\mu$ l/well. The cells were treated according to the aforementioned grouping strategy. After 48 h, 10  $\mu$ l CCK-8 solution (cat. no. C0041; Beyotime Institute of Biotechnology) was added to each well, and the cells were incubated for 2 h. The absorbance of each group of cells was measured using an automatic microplate reader (Biotek SynergyH4; Biotek; Agilent Technologies, Inc.).

**Transwell assay.** VSMCs in logarithmic growth phase were adjusted to a concentration of  $1 \times 10^5$  cells/ml. Subsequently, 150  $\mu$ l cell suspension was seeded in the upper chamber of a 24-well plate with a Transwell insert (pore size, 8  $\mu$ m). The lower chamber was filled with 10% serum-containing medium. After incubation at 37°C for 24 h, the cells in the upper chamber were gently removed using a sterile cotton swab. The cells that had migrated to the lower chamber were fixed in prepared 90% methanol solution for 30 min and stained with crystal violet for 30 min at room temperature. After air-drying, the cells were counted under a high-power light microscope (BX53; Olympus Corporation).

**Immunofluorescence.** VSMCs cultured in confocal cell culture dishes were fixed at room temperature with 4% paraformaldehyde for 20 min. After discarding the solution, the cells were treated with 0.2% Triton-100 solution at room temperature for 15 min to permeabilize the membrane. Subsequently, the cells were blocked with 5% bovine serum

albumin (MedChemExpress) solution at room temperature for 30 min and were incubated overnight at 4°C with primary antibodies against monocyte chemoattractant protein 1 (MCP-1; 1:1,000, cat. no. 26161-1-AP; Wuhan Sanying Biotechnology), vascular cell adhesion molecule 1 (VCAM-1; 1:1,000, cat. no. 11444-1-AP; Wuhan Sanying Biotechnology), SIRT1 (1:1,000, cat. no. ab189494; Abcam), p65 (1:1,000, cat. no. ab32536; Abcam) and PKH67 (cat. no. C3635S; Beyotime Institute of Biotechnology). Subsequently, the cells were incubated at room temperature for 2 h with Goat Anti-Rabbit IgG H&L (Alexa Fluor<sup>®</sup> 488) (1:1,000, cat. no. ab150077; Abcam) secondary antibodies. The cells were then incubated at room temperature with DAPI (cat. no. C1005; Beyotime Institute of Biotechnology) diluted solution for 10 min. Finally, 1 ml PBS was added, and the cells were observed and images were captured using a laser confocal microscope (BX53; Olympus Corporation).

**RT-qPCR.** Total RNA was extracted from VSMCs using TRIzol<sup>®</sup> (Invitrogen; Thermo Fisher Scientific, Inc.). The concentration and purity of RNA were determined by UV analysis. The RNA was reverse transcribed into cDNA using a RT kit (cat. no. RR037A; Takara Bio, Inc.) at 37°C for 15 min and 85°C for 5 sec. qPCR was performed according to the instructions of the SYBR Green kit (cat. no. FP205; Tiangen Biotech Co., Ltd.) under the following thermocycling conditions: Pre-denaturation at 95°C for 5 min, followed by 40 cycles of denaturation at 95°C for 20 sec, annealing at 60°C for 30 sec and extension at 72°C for 10 sec. The expression levels of the target genes were calculated using the  $2^{-\Delta\Delta C_q}$  method (31), with GAPDH used as the control gene. The primer sequences are shown in Table I.

**Animal model of AS.** A total of 20 male C57BL/6 mice (age, 6-8 weeks; weight, 18-22 g) were purchased from RayBiotech Life. The mice were maintained at a temperature of ~25°C, 55% humidity and under a 12-h light/dark cycle, with free access to food and water. After 1 week of acclimation, the mice were divided into a normal diet group and a high-fat diet (composition: 60% kcal from fat, 20% kcal from carbohydrates and 20% kcal from protein) group. The total feeding period was 12 weeks. After 12 weeks, the mice were divided into four groups: Control group, the high-fat diet (model) group, the model + MSC-exos group, and the model + Ba-exos group ( $n=5$  mice/group). The model + MSC-exos group and the model + Ba-exos group, which were injected with 150  $\mu$ g MSC-exos or Ba-exos twice a week, respectively. The control group mice were injected with saline twice a week. A high-fat diet was continued during the entire 16-week high-fat feeding period. Subsequently, 100  $\mu$ l blood was collected from the tail vein of mice immediately before sacrifice. The collected blood was allowed to clot at room temperature for 30 min, followed by centrifugation at  $3,000 \times g$  for 15 min at 4°C to separate the serum. The resulting serum was stored at -80°C until further analysis. Mouse serum was used for the detection of blood glucose, total cholesterol, LDL-cholesterol (LDL-C), high-density lipoprotein-cholesterol (HDL-C), triglycerides and uric acid levels using an automatic biochemical analyzer (BS-240VET; Shenzhen Mindray Bio-Medical Electronics Co., Ltd.). Subsequently, mice were euthanized by cervical dislocation, and the chest was opened

Table I. Primer sequences.

| Gene          | Forward, 5'-3'         | Reverse, 5'-3'        |
|---------------|------------------------|-----------------------|
| MCP-1         | CCACTCACCTGCTGCTACTCA  | TCCTTCTTGGGGTCAGCACA  |
| IL-6          | AGCCAGAGTCCTTCAGAGAGAT | AGCCACTCCTTCTGTGACTCC |
| VCAM-1        | AGTCCGTCTTGACCATGGAGC  | GGGGGCCACTGAATTGAATCT |
| ICAM-1        | CACATTCACGGTGCTGGCTA   | GGGTGTCGAGCTTTGGGATG  |
| SIRT1         | AGCAGGTTGCAGGAATCCAA   | CACCTAGGGCACCAGGAAC   |
| IL-1 $\beta$  | ACCTGTGTCTTTCCCGTGGA   | GGAACGTCACACACCAGCAG  |
| TNF- $\alpha$ | GCCACCACGCTCTTCTGTC    | CTCCAGCTGCTCCTCCACT   |
| GAPDH         | AAATCAAGTGGGGCGATGCT   | AACATGGGGGCATCAGCAGA  |

ICAM-1, intercellular adhesion molecule 1; MCP-1, monocyte chemoattractant protein 1; VCAM-1, vascular cell adhesion molecule 1.

for dissection. The main arteries were isolated and rinsed. The aortic arch segment was fixed in 4% paraformaldehyde at 4°C for 24 h, then embedded in paraffin at 60°C for 2 h and cut into 4- $\mu$ m sections. For Oil Red O staining, the sections were stained with 0.5% Oil Red O solution (cat. no. G1015-100ML; Wuhan Servicebio Technology Co., Ltd.) for 15 min at room temperature, then counterstained with hematoxylin for 1 min. For Masson's trichrome staining (cat. no. G1006; Wuhan Servicebio Technology Co., Ltd.), the sections were stained with Weigert's iron hematoxylin for 10 min, differentiated with phosphomolybdic-phosphotungstic acid for 5 min and stained with aniline blue for 5 min, all at room temperature (25°C). Images of the stained sections were captured using a light microscope (BX53; Olympus Corporation). The animal experiment was approved by the Experimental Animal Ethics Review Committee of the Guangdong Work Injury Rehabilitation Hospital (approval no. GDWIRH2023043).

**Western blotting.** Total proteins were extracted from VSMCs and the arterial tissues derived from mice with high-fat diet-induced AS using lysis buffer (cat. no. C500005; Sangon Biotech Co., Ltd.). Exosomal proteins were extracted using lysis buffer (cat. no. C500005; Sangon Biotech Co., Ltd.) to lyse the exosomes, followed by centrifugation at 13,680  $\times$  g at 4°C for 5 min to remove insoluble debris. After quantifying the protein concentration in the supernatant using the BCA protein assay kit (cat. no. P0009; Beyotime Institute of Biotechnology), total protein was mixed with loading buffer and incubated at 100°C for 5 min. Depending on the molecular weight of the target protein, denatured cellular proteins (10–20  $\mu$ g) were separated by sodium dodecyl sulfate-polyacrylamide gel electrophoresis on 6–15% gels and were then transferred to polyvinylidene fluoride membranes. The membranes were blocked with 5% non-fat dry milk in Tris-buffered saline-Tween-20 (0.5%) for 2 h at room temperature. The membranes were incubated overnight at 4°C with primary antibodies against GAPDH (1:5,000; cat. no. 10494-1-AP; Wuhan Sanying Biotechnology), p65 (1:1,000; cat. no. ab32536; Abcam), phosphorylated (p)-p65 (1:1,000; cat. no. ab239882; Abcam), acetylated p65 (cat. no. 3045s; Cell Signaling Technology, Inc.), MCP-1 (1:1,000; cat. no. 26161-1-AP; Wuhan Sanying Biotechnology), IL-6 (1:1,000; cat. no. 21865-1-AP; Wuhan Sanying Biotechnology), VCAM-1 (1:1,000; cat. no. 11444-1-AP; Wuhan Sanying

Biotechnology), intercellular adhesion molecule 1 (ICAM-1; 1:1,000; cat. no. 16174-1-AP; Wuhan Sanying Biotechnology) and SIRT1 (1:1,000; cat. no. ab110304; Abcam). The next day, the membranes were incubated at room temperature for 1 h with the corresponding HRP-conjugated Goat Anti-Rabbit IgG(H+L) (1:8,000; cat. no. SA00001-2; Wuhan Sanying Biotechnology) and HRP-conjugated Goat Anti-Mouse IgG(H+L) (1:8,000; cat. no. SA00001-1; Wuhan Sanying Biotechnology) secondary antibodies. Chemiluminescence (cat. no. STP262; Seyotin) was used for visualization, and ImageJ (1.53K; National Institutes of Health) was used for analysis.

**Co-immunoprecipitation (co-IP).** Cells were lysed in RIPA buffer (cat. no. P0013B; Beyotime Institute of Biotechnology), and the lysates were collected. A total of 200  $\mu$ g lysate was used per IP reaction. The lysates were incubated with 1  $\mu$ g anti-SIRT1 (1:1,000; cat. no. ab189494; Abcam), anti-NF- $\kappa$ B p65 (1:1,000; cat. no. ab207297; Abcam) or IgG (cat. no. ab18443; 1:10,000; Abcam), and mixed thoroughly using a mixer at 4°C for 24 h. A total of 50  $\mu$ l protein A/G magnetic beads (cat. no. 10002D; Thermo Fisher Scientific, Inc.) were then added and incubated at 4°C overnight. Beads were collected by centrifugation at 16,000  $\times$  g at 4°C for 10 min. The beads were washed with 1 ml cold PBS, and the bound proteins were eluted by boiling. The samples were then eluted with SDS-PAGE sample buffer to dissociate the protein complexes from the antibodies. The eluted proteins were separated by SDS-PAGE, transferred to a PVDF membrane and probed with anti-NF- $\kappa$ B p65 and anti-SIRT1 antibodies for western blot analysis.

**ELISA detection of MCP-1, IL-6, VCAM-1 and ICAM-1 levels in mouse serum.** The mouse serum from each experimental group was collected, and the levels of MCP-1, IL-6, VCAM-1 and ICAM-1 were detected according to the instructions of the respective ELISA kits: MCP-1 (cat. no. PC125; Beyotime Institute of Biotechnology), IL-6 (cat. no. AF0201; Beyotime Institute of Biotechnology), VCAM-1 (cat. no. PV951; Beyotime Institute of Biotechnology) and ICAM-1 (cat. no. PI493; Beyotime Institute of Biotechnology).

**Statistical analysis.** GraphPad Prism (version 8.0; Dotmatics) was used for statistical analysis. Data are presented as the mean  $\pm$  SD of three replicates. Significance was assessed



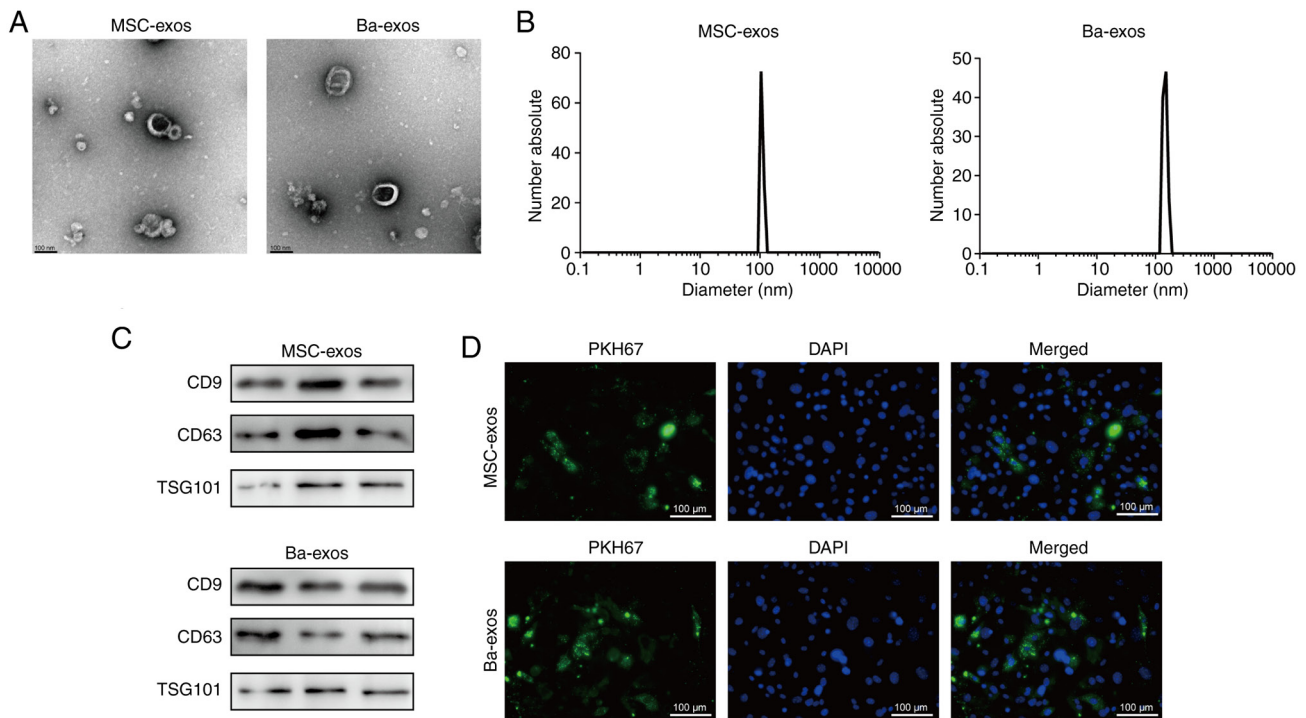


Figure 1. Separation and identification of exos. (A) Transmission electron microscope observation of the morphology of exos. (B) Nanoparticle tracking analysis of the particle size of exos. (C) Protein expression of the exo-specific proteins CD9, CD63 and TSG101. (D) Immunofluorescence analysis of vascular smooth muscle cells uptake of exos. n=3. Ba-exos, exos derived from baicalin-preconditioned MSCs; exos, exosomes; MSC-exos, MSC-derived exos; MSC, mesenchymal stem cell.

using the unpaired Student's t-test for two-group comparisons or one-way ANOVA with Tukey's multiple comparisons test for comparisons among three or more groups.  $P < 0.05$  was considered to indicate a statistically significant difference.

## Results

**Isolation and identification of exos.** Exos were isolated from MSCs and MSCs treated with Ba using differential ultracentrifugation. The morphology of purified exos was observed under TEM (Fig. 1A) and characteristic disc-like structures limited by a lipid bilayer were exhibited. The size distribution of exos was determined by NTA, which showed a diameter range of 70–200 nm (Fig. 1B). Western blotting confirmed the expression of the exo-specific markers CD9, CD63 and TSG101 (Fig. 1C). These results indicated the successful isolation of MSC-exos and Ba-exos. Subsequently, MSC-exos and Ba-exos were co-cultured with VSMCs, and immunofluorescence tracking results demonstrated that both MSC-exos and Ba-exos were efficiently internalized by VSMCs (Fig. 1D).

**Ba-exos inhibit the viability and migration of VSMCs.** Abnormal proliferation and migration of VSMCs are critical factors in accelerating the progression of AS (28). VSMCs were induced with ox-LDL to investigate the effects of Ba-exos on viability and migration. ox-LDL treatment significantly promoted the viability and migration of VSMCs, whereas treatment with MSC-exos and Ba-exos inhibited these abilities of VSMCs (Fig. 2A and B). Notably, Ba-exos exhibited a better inhibitory effect on VSMC viability and migration compared with MSC-exos treatment.

**Ba-exos inhibit NF- $\kappa$ B and alleviate inflammation in VSMCs.** Inflammation is a driving force in the progression of AS and late-stage AS plaque rupture (32); therefore, the effects of Ba-exos on inflammation in AS were investigated. The results of RT-qPCR demonstrated that the expression levels of the inflammatory genes IL-6, MCP-1, VCAM-1 and ICAM-1 were upregulated in VSMCs induced with ox-LDL, whereas treatment with MSC-exos reduced the expression levels of these genes compared with the ox-LDL group (Fig. 3A). Furthermore, treatment with Ba-exos further decreased the expression levels of IL-6, MCP-1, VCAM-1 and ICAM-1 in VSMCs compared with MSC-exos; however, no significant difference was observed in MCP-1 expression between the MSC-exos and Ba-exos groups. Immunofluorescence results confirmed these results; the expression levels of MCP-1 and VCAM-1 were elevated in ox-LDL-induced VSMCs, and were reversed in the MSC-exos and Ba-exos treatment groups (Fig. 3B). Furthermore, Ba-exos treatment significantly reduced the levels of MCP-1 and VCAM-1 in VSMCs compared with those in the MSC-exos group. These results revealed the inhibitory effects of Ba-exos on inflammation in VSMCs induced by ox-LDL. Additionally, a number of proinflammatory mediators, enzymes, chemokines and cytokines involved in AS can be regulated by the NF- $\kappa$ B transcription factor (33); therefore, the role of Ba-exos in inflammation in AS through NF- $\kappa$ B was investigated. Immunofluorescence results showed that treatment with MSC-exos and Ba-exos markedly inhibited ox-LDL-mediated NF- $\kappa$ B nuclear translocation in VSMCs, with a more pronounced effect observed in the Ba-exos group (Fig. 3C). Western blotting showed reduced acetylation levels of the NF- $\kappa$ B p65 subunit and decreased expression levels

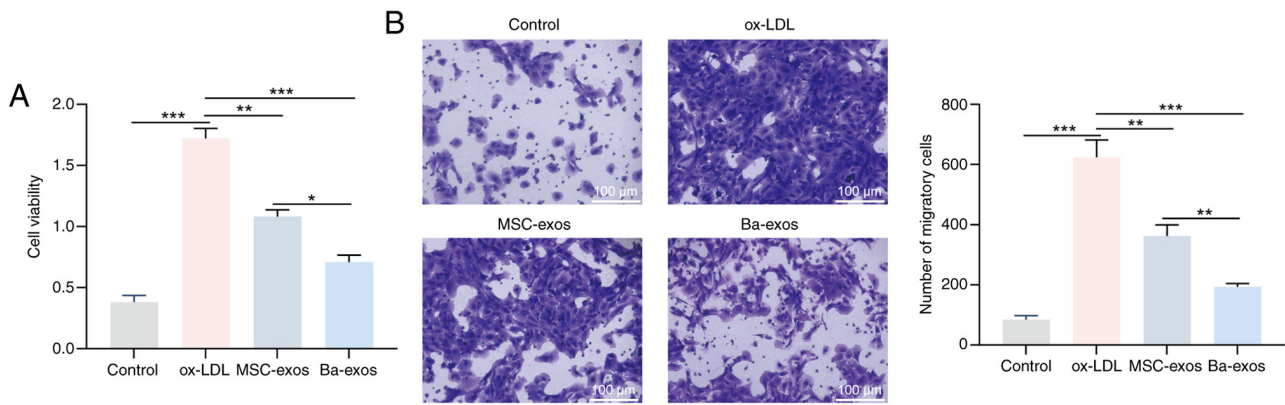


Figure 2. Ba-exos inhibit the viability and migration of VSMCs. (A) Cell Counting Kit-8 assay was performed to detect the viability of VSMCs. (B) Transwell assay was conducted to detect the migration of VSMCs.  $n=3$ . \* $P<0.05$ , \*\* $P<0.01$  and \*\*\* $P<0.001$ . Ba-exos, exos derived from baicalin-preconditioned MSCs; exos, exosomes; MSC-exos, MSC-derived exos; MSC, mesenchymal stem cell; ox-LDL, oxidized low-density lipoprotein; VSMCs, vascular smooth muscle cells.

of p-p65 in the MSC-exos and Ba-exos treatment groups compared with in the ox-LDL group, with a more prominent trend observed in the Ba-exos group (Fig. 3D and E). These results suggested that Ba-exos may inhibit NF- $\kappa$ B and alleviate inflammation in VSMCs.

*Ba-exos regulate the interaction between SIRT1 and NF- $\kappa$ B by upregulating SIRT1.* SIRT1 is a deacetylase that has been shown to inhibit NF- $\kappa$ B signaling by deacetylating the p65 subunit of NF- $\kappa$ B, thereby alleviating NF- $\kappa$ B-mediated inflammation (34). In the present study, the role of Ba-exos in regulating the SIRT1/NF- $\kappa$ B signaling pathway was investigated. The results of RT-qPCR revealed that the expression levels of SIRT1 were low in ox-LDL-induced VSMCs, which was reversed following treatment with MSC-exos and Ba-exos, with Ba-exos showing a more significant effect (Fig. 4A). Immunofluorescence results also validated this finding (Fig. 4B). To elucidate the mechanism of interaction between SIRT1 and NF- $\kappa$ B, the interaction between SIRT1 and NF- $\kappa$ B was confirmed through co-IP (Fig. 4C), and the co-expression of SIRT1 and NF- $\kappa$ B was further confirmed in VSMCs through immunofluorescence (Fig. 4D). These results indicated that Ba-exos may regulate the interaction between SIRT1 and NF- $\kappa$ B by upregulating SIRT1.

*Ba-exos alleviate inflammation, and inhibit the viability and migration of VSMCs by regulating SIRT1.* si-NC and si-SIRT1 were transfected into Ba-exos-treated VSMCs to further investigate the effect of Ba-exos on AS progression through SIRT1. The results of RT-qPCR showed that the mRNA expression levels of SIRT1 were reduced in the si-SIRT1 group compared with those in cells transfected with si-NC, indicating successful transfection of si-SIRT1 (Fig. S1). As shown in Fig. S2A and B, knocking down SIRT1 reversed the inhibitory effects of Ba-exos on the viability and migration of VSMCs, thus promoting their viability and migration. The results of RT-qPCR showed that silencing SIRT1 reversed the inhibitory effects of Ba-exos on the expression of inflammatory factors in VSMCs, upregulating the mRNA expression levels of IL-6, MCP-1, VCAM-1 and ICAM-1 in VSMCs (Fig. 5A). Immunofluorescence results also indicated that MCP-1 and VCAM-1 expression levels were decreased in the

Ba-exos-treated group, whereas this trend was significantly reversed following knockdown of SIRT1, although the difference was not significant (Fig. 5B). In addition, western blotting showed that, compared with those in the Ba-exos-treated group, the protein expression levels of IL-6, MCP-1, VCAM-1 and ICAM-1 were increased in VSMCs following SIRT1 knockdown, and the ratio of p-p65/p65 was also increased in VSMCs (Fig. 5C). In summary, these results suggested that Ba-exos may regulate SIRT1 to alleviate inflammation, and inhibit the viability and migration of VSMCs.

*Ba-exos alleviate AS progression in vivo.* Finally, the effect of Ba-exos on AS progression was investigated *in vivo*. The results revealed that the levels of blood glucose, total cholesterol, HDL-C, triglycerides and uric acid were increased, whereas the levels of LDL-C were decreased in the serum of the model group; by contrast, the levels of these indicators were reversed following treatment with MSC-exos and Ba-exos (Fig. 6A). Notably, compared with in the MSC-exos group, the levels of these indicators in the serum of mice were further reversed following Ba-exos treatment, but the difference was not significant. Oil red O and Masson staining results showed that the model group exhibited markedly increased lipid-containing lesions and obvious AS plaques in the aortic arch, which were reduced following treatment with MSC-exos and Ba-exos, with a further reduction in lesion and plaque area after Ba-exos treatment compared with MSC-exos (Fig. 6B and C). Furthermore, ELISA detected increased levels of MCP-1, IL-6, VCAM-1 and ICAM-1 in the serum of the model group, which were decreased following treatment with MSC-exos and further decreased after Ba-exos treatment compared with MSC-exos treatment, but the difference was not significant (Fig. 6D). Notably, western blotting results showed that MSC-exos and Ba-exos upregulated the expression levels of SIRT1 in the model group and lowered the ratio of p-p65/p65. However, no significant difference in SIRT1 expression was detected between the MSC-exos group and the model group. These trends were more pronounced in the Ba-exos treatment group (Fig. 6E). Concurrently, RT-qPCR and western blotting indicated that, compared with those in the model group, the expression levels of TNF- $\alpha$ , IL-1 $\beta$ , ICAM-1, MCP-1, VCAM-1 and IL-6 were significantly reduced in both

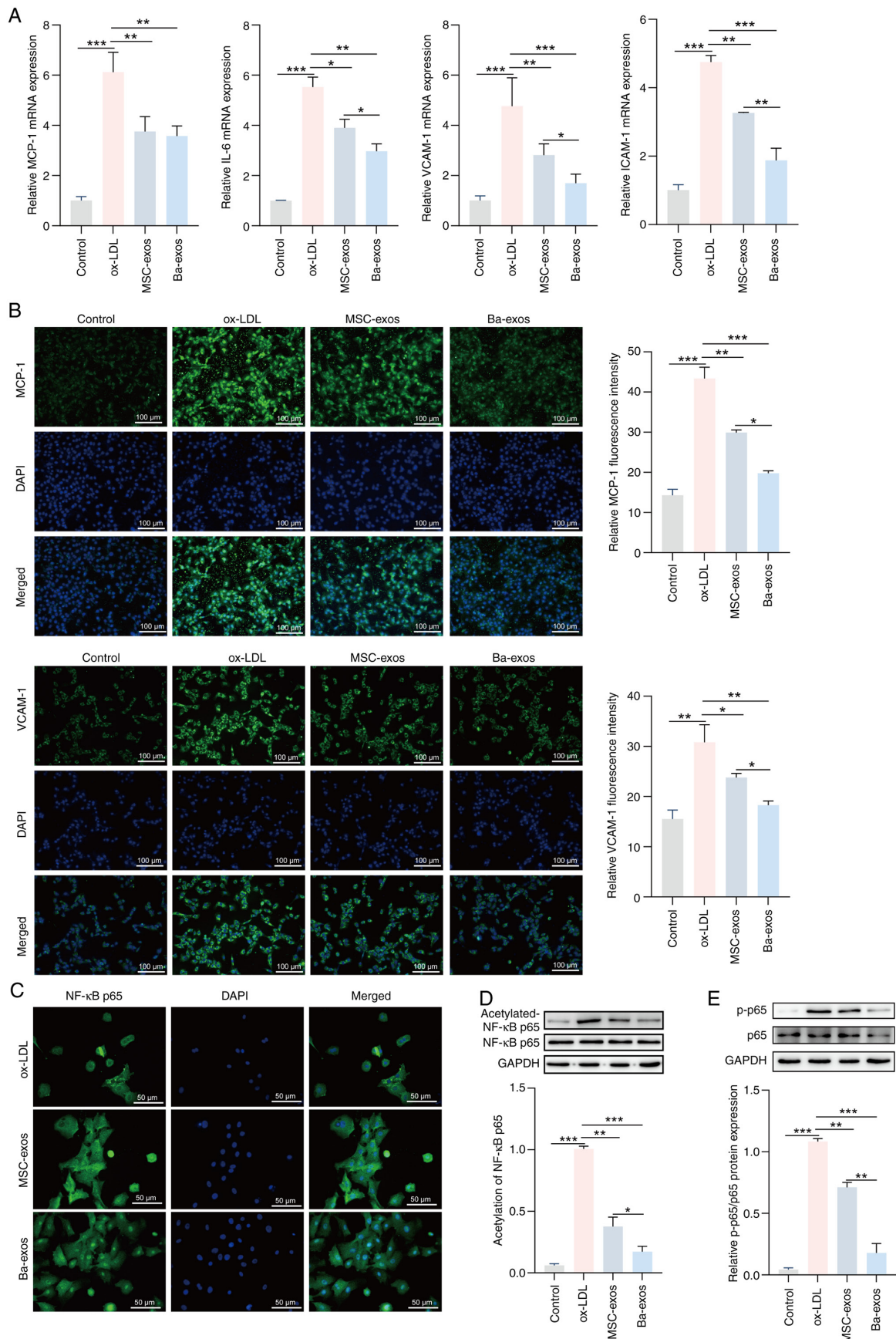


Figure 3. Ba-exos inhibit NF- $\kappa$ B activation and alleviate inflammation in VSMCs. (A) Reverse transcription-quantitative PCR was performed to detect the expression levels of the inflammatory genes MCP-1, IL-6, VCAM-1 and ICAM-1 in VSMCs. Immunofluorescence was used to detect the (B) levels of MCP-1 and VCAM-1, and (C) NF- $\kappa$ B nuclear translocation in VSMCs. Western blotting was performed to detect the (D) acetylation levels of NF- $\kappa$ B and the (E) protein expression levels of p65 and p-p65 in VSMCs. n=3. \*P<0.05, \*\*P<0.01 and \*\*\*P<0.001. Ba-exos, exos derived from baicalin-preconditioned MSCs; exos, exosomes; ICAM-1, intercellular adhesion molecule 1; MCP-1, monocyte chemoattractant protein 1; MSC-exos, MSC-derived exos; MSC, mesenchymal stem cell; ox-LDL, oxidized low-density lipoprotein; p-, phosphorylated; VCAM-1, vascular cell adhesion molecule 1; VSMCs, vascular smooth muscle cells.



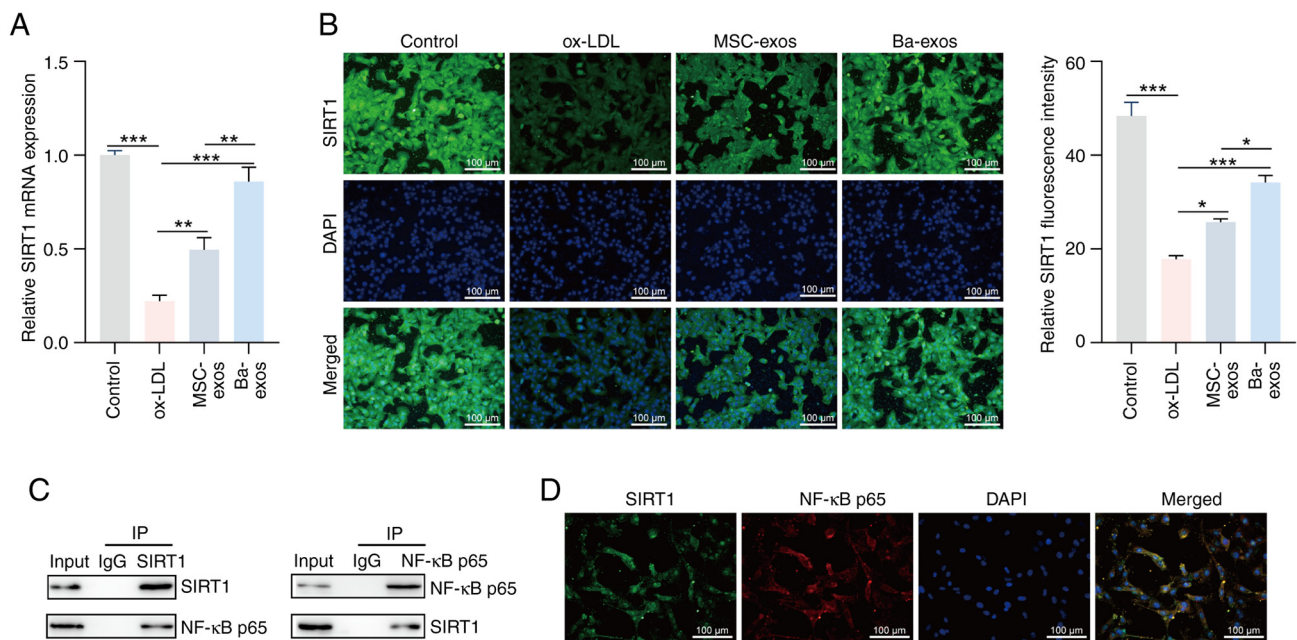


Figure 4. Ba-exos regulate the interaction between SIRT1 and NF- $\kappa$ B by upregulating SIRT1. (A) Reverse transcription-quantitative PCR was performed to detect the mRNA expression levels of SIRT1 in VSMCs. (B) Immunofluorescence was used to detect the levels of SIRT1 in VSMCs. (C) Co-IP analysis of the interaction between SIRT1 and NF- $\kappa$ B. (D) Immunofluorescence colocalization of SIRT1 and NF- $\kappa$ B expression in VSMCs.  $n=3$ . \* $P<0.05$ , \*\* $P<0.01$  and \*\*\* $P<0.001$ . Ba-exos, exos derived from baicalin-preconditioned MSCs; exos, exosomes; IP, immunoprecipitation; MSC-exos, MSC-derived exos; MSC, mesenchymal stem cell; ox-LDL, oxidized low-density lipoprotein; SIRT1, sirtuin 1; VSMCs, vascular smooth muscle cells.

the MSC-exos and Ba-exos groups, with the Ba-exos group showing a more pronounced effect (Fig. S3). In conclusion, Ba-exos may alleviate AS progression *in vivo* by regulating SIRT1/NF- $\kappa$ B.

## Discussion

In recent years, with changes in lifestyle, the incidence of AS has increased, leading to a larger number of patients with cardiovascular diseases, such as stroke, coronary heart disease and myocardial infarction, which severely threaten human life and health (35,36). Although current clinical treatments for AS exhibit a certain degree of effectiveness, there are toxic side effects and risks; therefore, there is a need to identify new therapeutic methods that are safe and effective with minimal side effects. MSCs are stem cells with multi-differentiation potential and self-renewal ability; due to their abundant sources and ease of culture and expansion, they have garnered interest in various research fields (37). In disease models, it has been shown that stem cells can exert their unique anti-inflammatory and immune-regulatory capabilities by secreting various bioactive substances in conditions such as coronary heart disease, Alzheimer's disease, fibrotic diseases and cancer (38-41). As a long-term inflammatory disease of blood vessels, AS may be markedly regulated by MSC-based therapies (42). In the present study, Ba-exos were isolated from Ba-pretreated MSCs, and the mechanism by which Ba-exos regulates the SIRT1/NF- $\kappa$ B signaling pathway to inhibit inflammation and exert protective effects on AS was explored.

The advantages of exos in treating various diseases have previously been confirmed (43,44). MSC-exos contain a rich array of bioactive substances, including miRNAs, cytokines and proteins, that can inhibit inflammation, regulate immune

cell activity and stimulate tissue regeneration through targeted delivery of these bioactive molecules (45). Research has shown that the substances carried by exos vary depending on the type of source cells and their state, such as transformation, differentiation, stimulation and stress (46). Notably, pretreated MSC-exos have been reported to enhance therapeutic and transplant efficacy. For example, exos derived from atorvastatin-pretreated MSCs have been shown to accelerate diabetic wound healing by enhancing angiogenesis through the AKT/eNOS pathway (30). Additionally, exos derived from TNF- $\alpha$ -pretreated gingival MSCs can enhance M2 macrophage polarization, inhibit inflammation and alleviate periodontitis (47). Furthermore, Ba has shown good therapeutic effects on cardiovascular diseases. Previous studies have revealed that Ba exhibits potential in treating AS and myocardial ischemia/reperfusion injury through anti-inflammatory, antioxidant and lipid metabolism mechanisms (48,49). Zhu *et al* (50) demonstrated that osteoclast-derived factors and exosomes containing miRNAs can enhance or inhibit osteoblast differentiation through paracrine and cell-contact mechanisms, suggesting a central coupling role in bone formation. Similarly, the present study explored the potential paracrine effects of Ba-exos on VSMCs through the regulation of inflammatory pathways, highlighting the therapeutic potential of exosome-based interventions in AS. Additionally, Zhao *et al* (51) and Zhang *et al* (52) have reported that Ba-exos may alleviate acute liver injury and improve ischemia/reperfusion injury, highlighting their therapeutic potential in tissue repair and regeneration. In the present study, it was hypothesized that intervening with Ba in MSC-exos may endow them with anti-inflammatory properties, thereby alleviating the progression of AS. As anticipated, it was revealed that Ba-exos significantly inhibited inflammation and alleviated

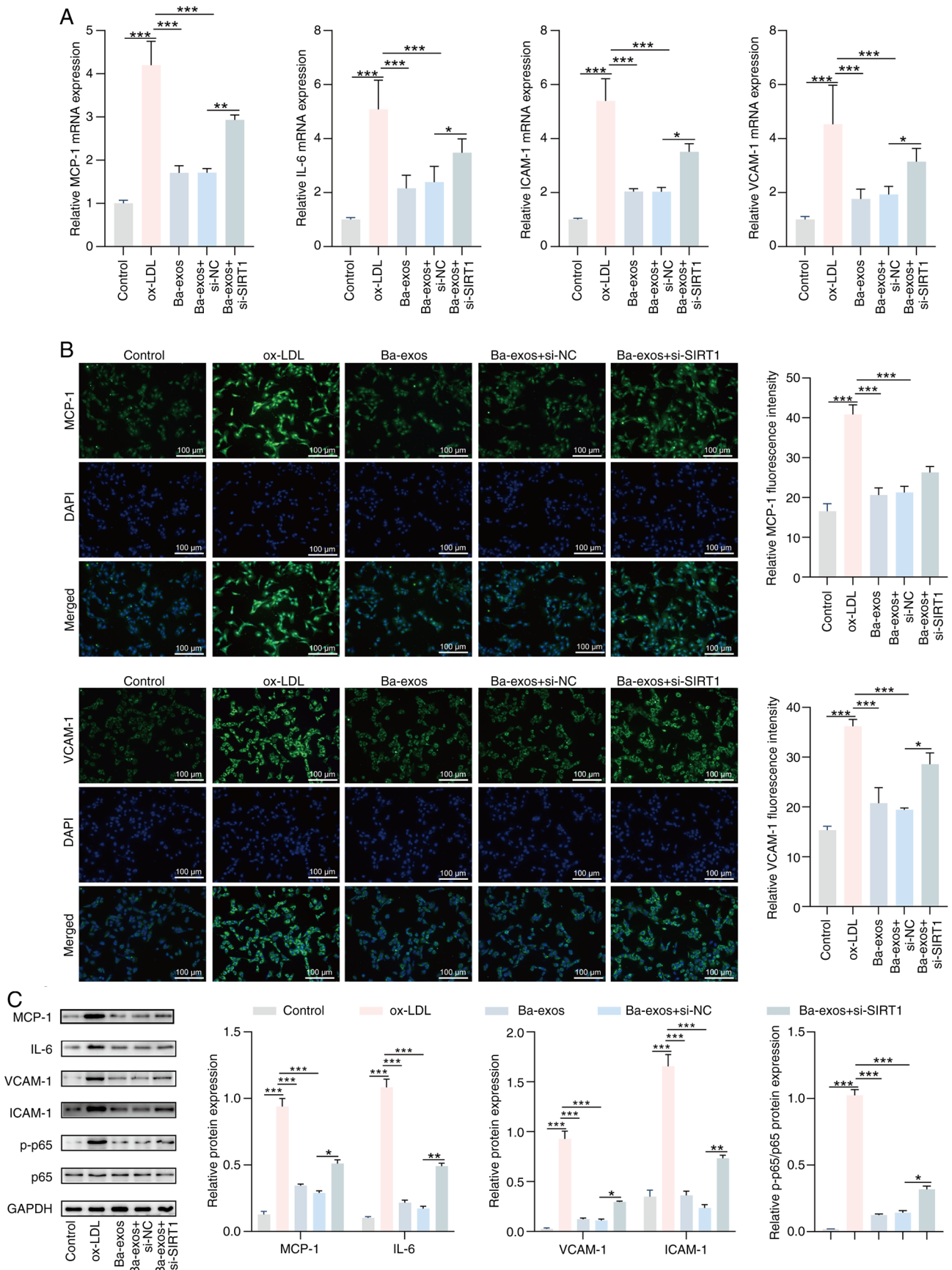


Figure 5. Ba-exos attenuate inflammation of VSMCs by regulating SIRT1. (A) Reverse transcription-quantitative PCR was performed to detect the expression of inflammatory genes MCP-1, IL-6, VCAM-1 and ICAM-1 in VSMCs. (B) Immunofluorescence was used to detect the levels of MCP-1 and VCAM-1 in VSMCs. (C) Western blotting was performed to detect the protein levels of MCP-1, IL-6, VCAM-1, ICAM-1, p65 and p-p65 in VSMCs.  $n=3$ . \* $P<0.05$ , \*\* $P<0.01$  and \*\*\* $P<0.001$ . Ba-exos, exos derived from baicalin-preconditioned MSCs; exos, exosomes; ICAM-1, intercellular adhesion molecule 1; MCP-1, monocyte chemoattractant protein 1; MSC-exos, MSC-derived exos; MSC, mesenchymal stem cell; NC, negative control; ox-LDL, oxidized low-density lipoprotein; p-, phosphorylated; si, small interfering RNA; SIRT1, sirtuin 1; VCAM-1, vascular cell adhesion molecule 1; VSMCs, vascular smooth muscle cells.



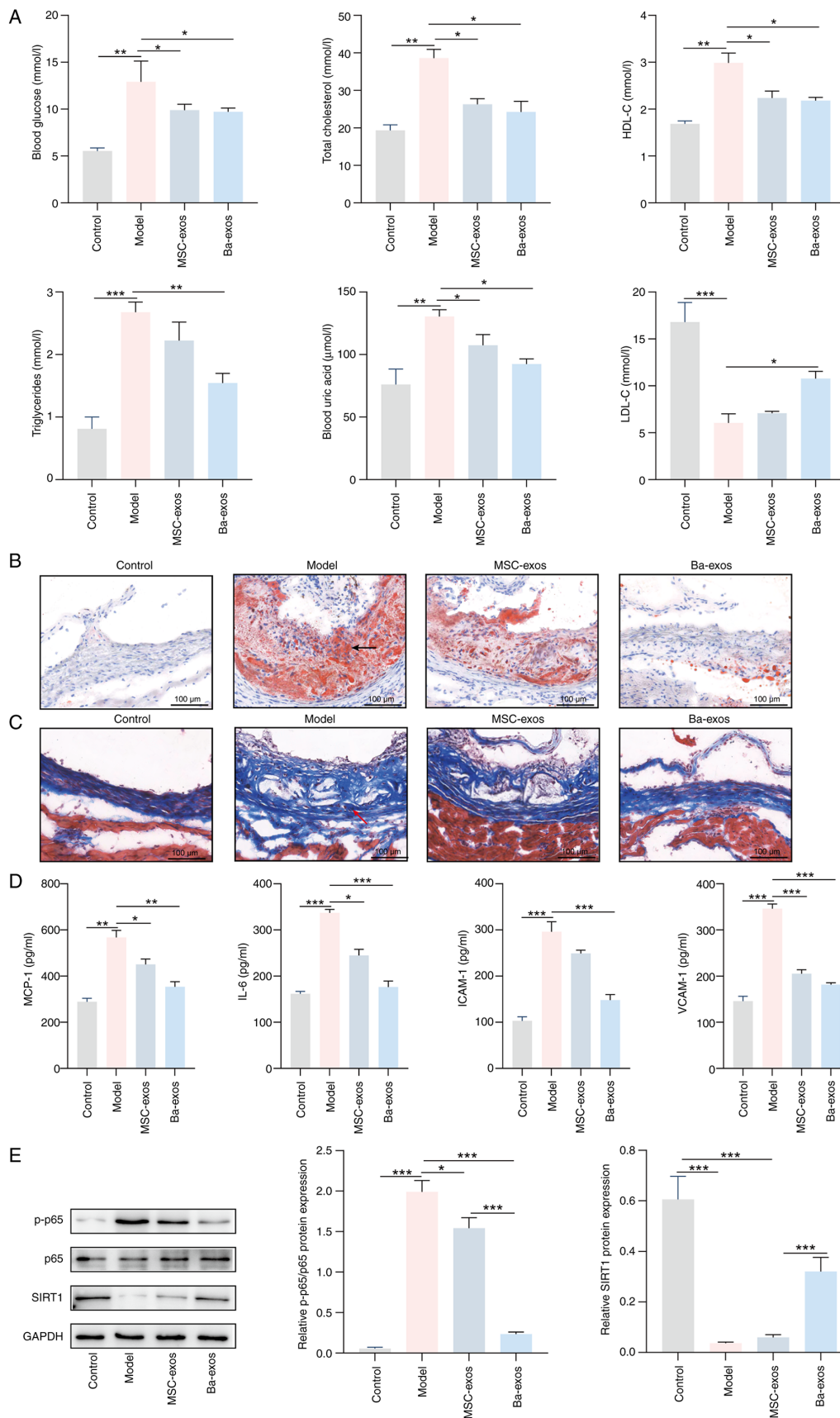


Figure 6. Ba-exos may alleviate the progression of atherosclerosis *in vivo* by regulating SIRT1/NF- $\kappa$ B. (A) Automatic biochemical analyzer was used to detect blood glucose, total cholesterol, LDL-C, HDL-C, triglycerides and uric acid levels in mouse serum. (B) Oil Red O staining (arrows indicate the locations of the lesions) and (C) Masson staining (arrows indicate the locations of the lesions) were performed to assess tissue pathology. (D) ELISA was used to detect the levels of MCP-1, IL-6, VCAM-1 and ICAM-1 in mouse serum. (E) Western blotting was used to detect the protein expression levels of SIRT1, p65 and p-p65 in mouse tissues.  $n=5$ .  $^{*}P<0.05$ ,  $^{**}P<0.01$  and  $^{***}P<0.001$ . Ba-exos, exos derived from baicalin-preconditioned MSCs; exos, exosomes; HDL-C, high-density lipoprotein-cholesterol; ICAM-1, intercellular adhesion molecule 1; MCP-1, monocyte chemoattractant protein 1; LDL-C, low-density lipoprotein-cholesterol; MSC-exos, MSC-derived exos; MSC, mesenchymal stem cell; p-, phosphorylated; SIRT1, sirtuin 1; VCAM-1, vascular cell adhesion molecule 1.

AS progression compared with MSC-exos. This result is consistent with the findings of a previous study that reported Ba-exos can alleviate acute liver injury (51). These findings indicated that Ba pretreatment may enhance the therapeutic efficacy of MSC-exos in diseases.

VSMCs are important components of the vascular wall, which are responsible for regulating vascular contraction and relaxation, while also secreting various vasoactive factors (53,54). Abnormal proliferation and migration of VSMCs are involved in plaque formation, and are key factors driving the progression of AS (55,56). An increasing number of studies have confirmed that exos serve a critical role in AS by regulating the proliferation and migration of VSMCs. For example, Guo *et al* (57) demonstrated that adipose tissue-derived exos can exacerbate the progression of AS by promoting the proliferation and migration of VSMCs within plaques. Liu *et al* (58) also reported that macrophage-derived exos induced by ox-LDL may promote the progression of AS by regulating the circ\_100696/miR-503-5p/PAPPA axis, which mediates VSMC proliferation and migration. Similarly, in the present study, it was shown that Ba-exos significantly inhibited ox-LDL-induced viability and migration of VSMCs. Notably, inflammatory factors expressed in VSMCs, such as MCP-1, VCAM-1 and ICAM-1, accelerate the progression of AS (59). Therefore, effectively blocking these proteins may suppress the development of AS. In the present study, it was revealed that Ba-exos could inhibit the ox-LDL-induced upregulation of the inflammatory genes IL-6, ICAM-1 and VCAM-1, and the chemokine MCP-1 in VSMCs. These results suggested that Ba-exos could alleviate the progression of AS by inhibiting VSMC viability and migration, and by downregulating cell inflammatory factors in VSMCs.

Inflammatory responses are closely related to AS, and NF- $\kappa$ B is a key target in controlling inflammation. The activation of NF- $\kappa$ B serves an important role in the occurrence and development of AS by enhancing the transcription of various proinflammatory cytokines (60). However, to the best of our knowledge, the potential protective effect of Ba-exos on AS related to the inhibition of NF- $\kappa$ B activation has not yet been reported. The results of the current study indicated that ox-LDL induced the phosphorylation of p65 in VSMCs, promoting the nuclear translocation of NF- $\kappa$ B, whereas the expression of NF- $\kappa$ B was significantly increased in AS tissues. However, these trends were reversed following treatment with Ba-exos. These findings suggested that Ba-exos may reduce the production of proinflammatory factors by inhibiting the activation of NF- $\kappa$ B in AS.

SIRT1 influences inflammation, apoptosis and other processes through the deacetylation of transcription factors, proteins and histones, acting as a regulator of inflammatory processes related to the deacetylation of NF- $\kappa$ B (61). SIRT1 interacts with the RelA/p65 subunit of NF- $\kappa$ B and inhibits NF- $\kappa$ B transcription by deacetylating the lysine 310 residue of this subunit (62). In the current study, an interaction between SIRT1 and NF- $\kappa$ B was identified, and treatment with Ba-exos significantly upregulated SIRT1 while reducing the acetylation levels of NF- $\kappa$ B p65. These findings indicated that Ba-exos may increase the deacetylation of NF- $\kappa$ B p65 by activating SIRT1, thereby lowering the expression of NF- $\kappa$ B p65 and inhibiting inflammation to alleviate AS. This is similar

to the findings of Wei *et al* (63), in which platelet-derived exos were shown to regulate endothelial cell inflammation in coronary thrombosis by promoting SIRT1 expression and inhibiting NF- $\kappa$ B transcription. In summary, the aforementioned results demonstrated that Ba-exos may alleviate AS by activating SIRT1 and inhibiting NF- $\kappa$ B transcription, thereby suppressing inflammation.

In conclusion, exos from MSCs and MSCs pretreated with Ba were successfully isolated. Compared with MSC-exos, Ba-exos markedly reduced the formation of AS plaques and decreased the lesion area by reducing the secretion of inflammatory factors in the mouse serum. Furthermore, Ba-exos significantly inhibited the viability and migration of ox-LDL-induced VSMCs, and suppressed the expression of the inflammatory factors MCP-1, IL-6, VCAM-1 and ICAM-1 in VSMCs compared with MSC-exos. Mechanistically, Ba-exos upregulated the expression of SIRT1, inhibited NF- $\kappa$ B activation and thus suppressed inflammation to alleviate AS progression. In summary, the results of the present study demonstrated that Ba-exos exhibit notable ability to inhibit AS progression, providing novel methods and perspectives for the clinical treatment of AS.

#### Acknowledgements

Not applicable.

#### Funding

The present study was supported by the National Natural Science Foundation of China (grant no. 62076103), the Guangdong Provincial Bureau of Traditional Chinese Medicine Foundation (grant no. 20241038), the Guangdong Province Key Areas Research and Development Plan (grant no. 2018B030339001) and the Guangdong Province General University Youth Innovative Talent Project (grant no. 2021KQNCX013).

#### Availability of data and materials

The data generated in the present study may be requested from the corresponding author.

#### Authors' contributions

XCY, YBH and WW conceived and designed the experiments. WTH, JFF, YLC, XYC and XLL analyzed and interpreted the data. YBH wrote the manuscript. All authors read and approved the final version of the manuscript. XCY and YBH confirm the authenticity of all the raw data.

#### Ethics approval and consent to participate

The animal experiments were approved by the Experimental Animal Ethics Review Committee of the Guangdong Work Injury Rehabilitation Hospital (approval no. GDWIRH2023043). The use of primary cells was approved by the Experimental Animal Ethics Review Committee of the Guangdong Work Injury Rehabilitation Hospital (approval no. GDWIRH2023044).

## Patient consent for publication

Not applicable.

## Competing interests

The authors declare that they have no competing interests.

## References

- Fan J and Watanabe T: Atherosclerosis: Known and unknown. *Pathol Int* 72: 151-160, 2022.
- Falk E: Pathogenesis of atherosclerosis. *J Am Coll Cardiol* 47 (8 Suppl): C7-C12, 2006.
- Arnett DK, Blumenthal RS, Albert MA, Buroker AB, Goldberger ZD, Hahn EJ, Himmelfarb CD, Khera A, Lloyd-Jones D, McEvoy JW, *et al*: 2019 ACC/AHA guideline on the primary prevention of cardiovascular disease: A report of the american college of cardiology/American heart association task force on clinical practice guidelines. *Circulation* 140: e596-e646, 2019.
- Grundy SM, Stone NJ, Bailey AL, Beam C, Birtcher KK, Blumenthal RS, Braun LT, de Ferranti S, Faiella-Tommasino J, Forman DE, *et al*: 2018 AHA/ACC/AACVPR/AAPA/ABC/ACPM/ADA/AGS/APhA/ASPC/NLA/PCNA guideline on the management of blood cholesterol: A report of the american college of cardiology/American heart association task force on clinical practice guidelines. *Circulation* 139: e1082-e1143, 2019.
- Collet JP, Thiele H, Barbato E, Barthélémy O, Bauersachs J, Bhatt DL, Dendale P, Dorobantu M, Edvardsen T, Flügge T, *et al*: 2020 ESC guidelines for the management of acute coronary syndromes in patients presenting without persistent ST-segment elevation. *Eur Heart J* 42: 1289-1367, 2021.
- Aprosoaie AC, Costache AD and Costache II: Therapeutic strategies and chemoprevention of atherosclerosis: What do we know and where do we go? *Pharmaceutics* 14: 722, 2022.
- Capodanno D, Alberts M and Angiolillo DJ: Antithrombotic therapy for secondary prevention of atherothrombotic events in cerebrovascular disease. *Nat Rev Cardiol* 13: 609-622, 2016.
- Lan W, Petznick A, Heryati S, Rifada M and Tong L: Nuclear factor- $\kappa$ B: central regulator in ocular surface inflammation and diseases. *Ocul Surf* 10: 137-148, 2012.
- Baker RG, Hayden MS and Ghosh S: NF- $\kappa$ B, inflammation, and metabolic disease. *Cell Metab* 13: 11-22, 2011.
- Lawrence T: The nuclear factor NF- $\kappa$ B pathway in inflammation. *Cold Spring Harb Perspect Biol* 1: a001651, 2009.
- Wang D, Yu X, Gao K, Li F, Li X, Pu H, Zhang P, Guo S and Wang W: Sweroside alleviates pressure overload-induced heart failure through targeting CaMKII $\delta$  to inhibit ROS-mediated NF- $\kappa$ B/NLRP3 in cardiomyocytes. *Redox Biol* 74: 103223, 2024.
- Hao T, Fang W, Xu D, Chen Q, Liu Q, Cui K, Cao X, Li Y, Mai K and Ai Q: Phosphatidylethanolamine alleviates OX-LDL-induced macrophage inflammation by upregulating autophagy and inhibiting NLRP1 inflammasome activation. *Free Radic Biol Med* 208: 402-417, 2023.
- Huang D, Gao W, Lu H, Qian JY and Ge JB: Oxidized low-density lipoprotein stimulates dendritic cells maturation via LOX-1-mediated MAPK/NF- $\kappa$ B pathway. *Braz J Med Biol Res* 54: e11062, 2021.
- Bian W, Jing X, Yang Z, Shi Z, Chen R, Xu A, Wang N, Jiang J, Yang C, Zhang D, *et al*: Downregulation of LncRNA NORAD promotes Ox-LDL-induced vascular endothelial cell injury and atherosclerosis. *Aging (Albany NY)* 12: 6385-6400, 2020.
- Hwang JW, Yao H, Caito S, Sundar IK and Rahman I: Redox regulation of SIRT1 in inflammation and cellular senescence. *Free Radic Biol Med* 61: 95-110, 2013.
- Stein S, Schäfer N, Breitenstein A, Besler C, Winnik S, Lohmann C, Heinrich K, Brokopp CE, Handschin C, Landmesser U, *et al*: SIRT1 reduces endothelial activation without affecting vascular function in ApoE $^{-/-}$  mice. *Aging (Albany NY)* 2: 353-360, 2010.
- Yang Z, Li T, Wang C, Meng M, Tan S and Chen L: Dihydromyricetin inhibits M1 macrophage polarization in atherosclerosis by modulating miR-9-mediated SIRT1/NF- $\kappa$ B signaling pathway. *Mediators Inflamm* 2023: 2547588, 2023.
- Golpanian S, Wolf A, Hatzistergos KE and Hare JM: Rebuilding the damaged heart: Mesenchymal stem cells, cell-based therapy, and engineered heart tissue. *Physiol Rev* 96: 1127-1168, 2016.
- Ha DH, Kim HK, Lee J, Kwon HH, Park GH, Yang SH, Jung JY, Choi H, Lee JH, Sung S, *et al*: Mesenchymal stem/stromal cell-derived exosomes for immunomodulatory therapeutics and skin regeneration. *Cells* 9: 1157, 2020.
- Zhang N, Luo Y, Zhang H, Zhang F, Gao X and Shao J: Exosomes derived from mesenchymal stem cells ameliorate the progression of atherosclerosis in ApoE $^{-/-}$  mice via FENRRR. *Cardiovasc Toxicol* 22: 528-544, 2022.
- Ma J, Chen L, Zhu X, Li Q, Hu L and Li H: Mesenchymal stem cell-derived exosomal miR-21a-5p promotes M2 macrophage polarization and reduces macrophage infiltration to attenuate atherosclerosis. *Acta Biochim Biophys Sin (Shanghai)* 53: 1227-1236, 2021.
- Hu C and Li L: Preconditioning influences mesenchymal stem cell properties in vitro and in vivo. *J Cell Mol Med* 22: 1428-1442, 2018.
- Liu X, Wang J, Wang P, Zhong L, Wang S, Feng Q, Wei X and Zhou L: Hypoxia-pretreated mesenchymal stem cell-derived exosomes-loaded low-temperature extrusion 3D-printed implants for neural regeneration after traumatic brain injury in canines. *Front Bioeng Biotechnol* 10: 1025138, 2022.
- Li T, Zhao Y, Cao Z, Shen Y, Chen J, Huang X, Shao Z, Zeng Y, Chen Q, Yan X, *et al*: Exosomes Derived from apelin-pretreated mesenchymal stem cells ameliorate sepsis-induced myocardial dysfunction by alleviating cardiomyocyte pyroptosis via delivery of miR-34a-5p. *Int J Nanomedicine* 20: 687-703, 2025.
- Zhu J, Wang J, Sheng Y, Zou Y, Bo L, Wang F, Lou J, Fan X, Bao R, Wu Y, *et al*: Baicalin improves survival in a murine model of polymicrobial sepsis via suppressing inflammatory response and lymphocyte apoptosis. *PLoS One* 7: e35523, 2012.
- Motoo Y and Sawabu N: Antitumor effects of saikosaponins, baicalin and baicalein on human hepatoma cell lines. *Cancer Lett* 86: 91-95, 1994.
- Yu H, Chen B and Ren Q: Baicalin relieves hypoxia-aroused H9c2 cell apoptosis by activating Nrf2/HO-1-mediated HIF1 $\alpha$ /BNIP3 pathway. *Artif Cells Nanomed Biotechnol* 47: 3657-3663, 2019.
- Chen Z, Pan X, Sheng Z, Yan G, Chen L and Ma G: Baicalin suppresses the proliferation and migration of Ox-LDL-VSMCs in atherosclerosis through upregulating miR-126-5p. *Biol Pharm Bull* 42: 1517-1523, 2019.
- Wu Y, Wang F, Fan L, Zhang W, Wang T, Du Y and Bai X: Baicalin alleviates atherosclerosis by relieving oxidative stress and inflammatory responses via inactivating the NF- $\kappa$ B and p38 MAPK signaling pathways. *Biomed Pharmacother* 97: 1673-1679, 2018.
- Yu M, Liu W, Li J, Lu J, Lu H, Jia W and Liu F: Exosomes derived from atorvastatin-pretreated MSC accelerate diabetic wound repair by enhancing angiogenesis via AKT/eNOS pathway. *Stem Cell Res Ther* 11: 350, 2020.
- Livak KJ and Schmittgen TD: Analysis of relative gene expression data using real-time quantitative PCR and the 2 $^{-\Delta\Delta C_T}$  method. *Methods* 25: 402-408, 2001.
- Kong P, Cui ZY, Huang XF, Zhang DD, Guo RJ and Han M: Inflammation and atherosclerosis: Signaling pathways and therapeutic intervention. *Signal Transduct Target Ther* 7: 131, 2022.
- Zhang W, Yan C, Xiao Y, Sun Y, Lin Y, Li Q and Cai W: Sulfasalazine induces autophagy inhibiting neointimal hyperplasia following carotid artery injuries in mice. *Front Bioeng Biotechnol* 11: 1199785, 2023.
- Zheng Z, Bian Y, Zhang Y, Ren G and Li G: Metformin activates AMPK/SIRT1/NF- $\kappa$ B pathway and induces mitochondrial dysfunction to drive caspase3/GSDME-mediated cancer cell pyroptosis. *Cell Cycle* 19: 1089-1104, 2020.
- He B, Nie Q, Wang F, Han Y, Yang B, Sun M, Fan X, Ye Z, Liu P and Wen J: Role of pyroptosis in atherosclerosis and its therapeutic implications. *J Cell Physiol* 236: 7159-7175, 2021.
- Groenen AG, Halmos B, Tall AR and Westerterp M: Cholesterol efflux pathways, inflammation, and atherosclerosis. *Crit Rev Biochem Mol Biol* 56: 426-439, 2021.
- Lotfy A, AboQuella NM and Wang H: Mesenchymal stromal/stem cell (MSC)-derived exosomes in clinical trials. *Stem Cell Res Ther* 14: 66, 2023.
- Xiong J, Hu H, Guo R, Wang H and Jiang H: Mesenchymal stem cell exosomes as a new strategy for the treatment of diabetes complications. *Front Endocrinol (Lausanne)* 12: 646233, 2021.

39. Guo M, Yin Z, Chen F and Lei P: Mesenchymal stem cell-derived exosome: A promising alternative in the therapy of Alzheimer's disease. *Alzheimers Res Ther* 12: 109, 2020.
40. Chen W, Lin F, Feng X, Yao Q, Yu Y, Gao F, Zhou J, Pan Q, Wu J, Yang J, *et al*: MSC-derived exosomes attenuate hepatic fibrosis in primary sclerosing cholangitis through inhibition of Th17 differentiation. *Asian J Pharm Sci* 19: 100889, 2024.
41. Liu J, Ren L, Li S, Li W, Zheng X, Yang Y, Fu W, Yi J, Wang J and Du G: The biology, function, and applications of exosomes in cancer. *Acta Pharm Sin B* 11: 2783-2797, 2021.
42. Jiang Y, Yu M, Song ZF, Wei ZY, Huang J and Qian HY: Targeted delivery of mesenchymal stem cell-derived bioinspired exosome-mimetic nanovesicles with platelet membrane fusion for atherosclerotic treatment. *Int J Nanomedicine* 19: 2553-2571, 2024.
43. Liu S, Fan M, Xu JX, Yang LJ, Qi CC, Xia QR and Ge JF: Exosomes derived from bone-marrow mesenchymal stem cells alleviate cognitive decline in AD-like mice by improving BDNF-related neuropathology. *J Neuroinflammation* 19: 35, 2022.
44. Xu S, Cheuk YC, Jia Y, Chen T, Chen J, Luo Y, Cao Y, Guo J, Dong L, Zhang Y, *et al*: Bone marrow mesenchymal stem cell-derived exosomal miR-21a-5p alleviates renal fibrosis by attenuating glycolysis by targeting PFKM. *Cell Death Dis* 13: 876, 2022.
45. Gao L, Qiu F, Cao H, Li H, Dai G, Ma T, Gong Y, Luo W, Zhu D, Qiu Z, *et al*: Therapeutic delivery of microRNA-125a-5p oligonucleotides improves recovery from myocardial ischemia/reperfusion injury in mice and swine. *Theranostics* 13: 685-703, 2023.
46. Li M, Li S, Du C, Zhang Y, Li Y, Chu L, Han X, Galons H, Zhang Y, Sun H and Yu P: Exosomes from different cells: Characteristics, modifications, and therapeutic applications. *Eur J Med Chem* 207: 112784, 2020.
47. Nakao Y, Fukuda T, Zhang Q, Sanui T, Shinjo T, Kou X, Chen C, Liu D, Watanabe Y, Hayashi C, *et al*: Exosomes from TNF- $\alpha$ -treated human gingiva-derived MSCs enhance M2 macrophage polarization and inhibit periodontal bone loss. *Acta Biomater* 122: 306-324, 2021.
48. Liu R, Cao H, Zhang S, Cai M, Zou T, Wang G, Zhang D, Wang X, Xu J, Deng S, *et al*: ZBP1-mediated apoptosis and inflammation exacerbate steatotic liver ischemia/reperfusion injury. *J Clin Invest* 134: e180451, 2024.
49. Xu M, Li X and Song L: Baicalin regulates macrophages polarization and alleviates myocardial ischaemia/reperfusion injury via inhibiting JAK/STAT pathway. *Pharm Biol* 58: 655-663, 2020.
50. Zhu S, Yao F, Qiu H, Zhang G, Xu H and Xu J: Coupling factors and exosomal packaging microRNAs involved in the regulation of bone remodelling. *Biol Rev Camb Philos Soc* 93: 469-480, 2018.
51. Zhao S, Huang M, Yan L, Zhang H, Shi C, Liu J, Zhao S, Liu H and Wang B: Exosomes derived from baicalin-pretreated mesenchymal stem cells alleviate hepatocyte ferroptosis after acute liver injury via the Keap1-NRF2 pathway. *Oxid Med Cell Longev* 2022: 8287227, 2022.
52. Zhang B, Su L, Chen Z, Wu M, Wei J and Lin Y: Exosomes derived from baicalin-pretreated bone mesenchymal stem cells improve Th17/Treg imbalance after hepatic ischemia-reperfusion via FGF21 and the JAK2/STAT3 pathway. *IUBMB Life* 76: 534-547, 2024.
53. Pryma CS, Ortega C, Dubland JA and Francis GA: Pathways of smooth muscle foam cell formation in atherosclerosis. *Curr Opin Lipidol* 30: 117-124, 2019.
54. Grootaert MOJ, Finigan A, Figg NL, Uryga AK and Bennett MR: SIRT6 protects smooth muscle cells from senescence and reduces atherosclerosis. *Circ Res* 128: 474-491, 2021.
55. Zhu J, Liu B, Wang Z, Wang D, Ni H, Zhang L and Wang Y: Exosomes from nicotine-stimulated macrophages accelerate atherosclerosis through miR-21-3p/PTEN-mediated VSMC migration and proliferation. *Theranostics* 9: 6901-6919, 2019.
56. Li H, Zhuang W, Xiong T, Park WS, Zhang S, Zha Y, Yao J, Wang F, Yang Y, Chen Y, *et al*: Nrf2 deficiency attenuates atherosclerosis by reducing LOX-1-mediated proliferation and migration of vascular smooth muscle cells. *Atherosclerosis* 347: 1-16, 2022.
57. Guo B, Zhuang TT, Li CC, Li F, Shan SK, Zheng MH, Xu QS, Wang Y, Lei LM, Tang KX, *et al*: MiRNA-132/212 encapsulated by adipose tissue-derived exosomes worsen atherosclerosis progression. *Cardiovasc Diabetol* 23: 331, 2024.
58. Liu J, Zhang X, Yu Z and Zhang T: Exosomes promote atherosclerosis progression by regulating Circ\_100696/miR-503-5p/PAPPA axis-mediated vascular smooth muscle cells proliferation and migration. *Int Heart J* 64: 918-927, 2023.
59. Park JY, Park HM, Kim S, Jeon KB, Lim CM, Hong JT and Yoon DY: Human IL-320A94V mutant attenuates monocyte-endothelial adhesion by suppressing the expression of ICAM-1 and VCAM-1 via binding to cell surface receptor integrin  $\alpha$ V $\beta$ 3 and  $\alpha$ V $\beta$ 6 in TNF- $\alpha$ -stimulated HUVECs. *Front Immunol* 14: 1160301, 2023.
60. Feng X, Du M, Li S, Zhang Y, Ding J, Wang J, Wang Y and Liu P: Hydroxysafflor yellow A regulates lymphangiogenesis and inflammation via the inhibition of PI3K on regulating AKT/mTOR and NF- $\kappa$ B pathway in macrophages to reduce atherosclerosis in ApoE-/- mice. *Phytomedicine* 112: 154684, 2023.
61. Morigi M, Perico L and Benigni A: Sirtuins in renal health and disease. *J Am Soc Nephrol* 29: 1799-1809, 2018.
62. Kauppinen A, Suuronen T, Ojala J, Kaarniranta K and Salminen A: Antagonistic crosstalk between NF- $\kappa$ B and SIRT1 in the regulation of inflammation and metabolic disorders. *Cell Signal* 25: 1939-1948, 2013.
63. Wei K, Yu L, Li J, Gao J, Chen L, Liu M, Zhao X, Li M, Shi D and Ma X: Platelet-derived exosomes regulate endothelial cell inflammation and M1 macrophage polarization in coronary artery thrombosis via modulating miR-34a-5p expression. *Sci Rep* 14: 17429, 2024.



Copyright © 2025 Yang et al. This work is licensed under a Creative Commons Attribution-NonCommercial-NoDerivatives 4.0 International (CC BY-NC-ND 4.0) License.